03,09

Thermal annealing of CdTe-rich HgCdTe: structural and optical studies

© M.S. Ruzhevich[1], K.D. Mynbaev[2], N.L. Bazhenov[2], M.V. Dorogov[1], A.M. Smirnov[1], V.V. Belkov[2], M.V. Tomkovich[2], V.S. Varavin[3], V.G. Remesnik[3], I.N. Uzhakov[3], N.N. Mikhailov[3]

[1] ITMO University,
St. Petersburg, Russia
[2] Ioffe Institute,
St. Petersburg, Russia
[3] Rzhanov Institute of Semiconductor Physics, Siberian Branch, Russian Academy of Sciences,
Novosibirsk, Russia

E-mail: max.ruzhevich@niuitmo.ru

Received October 10, 2024
Revised November 17, 2024
Accepted November 18, 2024

The article presents the results of studying the structural and optical properties of $Hg_{1-x}Cd_xTe$ films with a high ($x = 0.5-0.7$) CdTe content, grown by molecular beam epitaxy and subjected to thermal annealing at temperatures from 330 to 440 °C. The effect of annealing on the crystal structure and point defects is determined based on optical transmittance, photoluminescence, X-ray diffraction, and energy-dispersive X-ray spectroscopy studies. It is shown that the defect structure of the material undergoes significant changes after annealing, while its crystalline perfection changes insignificantly.

Keywords: HgCdTe, annealing, photoluminescence, defects, structural properties.

DOI: 10.61011/PSS.2025.01.60575.4-25

1. Introduction

Solid solutions of $Hg_{1-x}Cd_xTe$ (CdHgTe) with a high ($x \geq 0.5$) CdTe content are used in the development of near-infrared photodetectors for astronomical observations [1] and in the creation of barrier layers of laser heterostructures [2] and *n*B*n*-photodetectors [3,4]. A material with a hole type of conductivity is required for the manufacture of both photodetectors and injection lasers, however, the acceptor doping of CdHgTe with $x \geq 0.5$ has not been sufficiently developed at the moment [5,6]. An obvious (and traditional for CdHgTe with $x < 0.5$) variant of such doping is the introduction of intrinsic acceptors such as mercury vacancies by thermal annealing under conditions of its deficiency [7]. However, for CdHgTe with $x \geq 0.5$, synthesized by the most popular method of molecular beam epitaxy(MBE) today, such annealing should be carried out at temperatures exceeding the growth temperature by 2–2.5 times. This can lead to structural changes and the appearance of a large number of defects in a material with weak chemical bonds, such as CdHgTe. We investigated these effects by studying the structural and optical properties of MBE-grown $Hg_{1-x}Cd_xTe$ films with $x = 0.5-0.7$ subjected to thermal annealing to generate mercury vacancies.

2. Experimental methods

Films with a thickness of $3-4\,\mu$m were grown on (013) GaAs [8] substrates and had a constant composition (determined by *in situ* ellipsometry) across thickness. The films were grown under conditions close to optimal for each composition, i. e. the substrate temperature decreased from a material with a higher x to a material with lower one. The films had a *n*-type of conductivity with an electron concentration immediately after growing, according to a study of the Hall effect at a temperature of $T = 77$ K, $(3-60) \cdot 10^{14}$ cm^{-3}. Annealing to generate vacancies was carried out at a temperature of T_{ann} from 330 to 440 °C (depending on the composition) in a helium atmosphere at a reduced mercury vapor pressure for 7–15 min. As a result, the films were converted to the *p*-type of conductivity with a hole concentration of $(2-7) \cdot 10^{15}$ cm^{-3}.

The as-grown and annealed films were studied by optical transmittance (OT), photoluminescence (PL), X-ray diffraction (XRD), and electron microscopy with energy-dispersive X-ray spectroscopy (EDX). The OT spectra were recorded at a temperature of $T = 294$ K using InfraLUM-801 Fourier spectrometer with a short-wave unit, or PerkinElmer Lambda 1050 grating spectrometer. PL spectra were recorded at $T = 103$ K and $T = 294$ K using MDR-23 monochromator with excitation by a semiconductor laser (wavelength $\lambda = 1.03\,\mu$m) and recording the signal with a germanium photodiode using lock-in detection. For comparison, the optical properties of CdHgTe samples grown by solid-state recrystallization with replenishment from the solid phase (volumetric growth) and liquid-phase epitaxy (LPE) were studied under the same conditions. X-ray diffraction patterns of the films were recorded using DRON-8 installation in a slit configuration with a BSV-29 sharp-focus tube with a copper anode and a NaI(Tl)

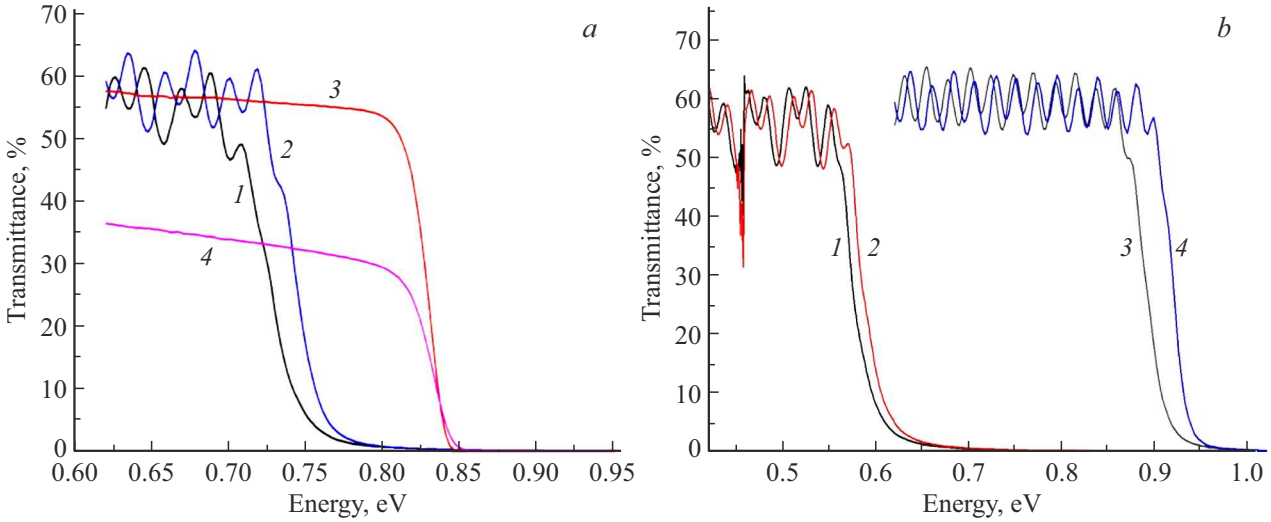

Figure 1. Optical transmittance spectra of the film ($T = 294$ K) with $x = 0.60$ before (*1*) and after (*2*) annealing, crystal sample (*3*) and a layer grown by the LPE method (*4*) (*a*); and samples of films with $x = 0.50$ (*1* and *2*) and $x = 0.70$ (*3* and *4*) before (*1* and *3*) and after (*2* and *4*) annealing (*b*).

Table 1. Changes of the spectral characteristics of films after annealing

Composition x	Optical transmittance edge shift, meV	PL peak shift, meV		ΔPL peak FWHM, meV	
	294 K	294 K	103 K	294 K	103 K
0.50	8–11	2–12	10–12	1–2	1–4
0.60	17–20	1–2	7–8	1–2	8–10
0.70	20–30	20–27	32–45	1–7	12–18

scintillation detector. EDX studies were carried out using a FEI Quanta 200 electron microscope.

3. Results and discussion

Figure 1 shows examples of OT spectra of a number of samples before and after thermal annealing. The spectra are typical of films grown by the MBE [9,10] method; in the low-energy part, they are characterized by pronounced interference fringes, indicating good planarity. To describe the sharpness of the transmittance edge, one can introduce the value ΔE, which is a segment on the axis of the abscissa equal to the energy difference between the maximum and the intersection with the axis of the abscissa of the tangent drawn through the point where the transmittance drops by a factor of two for each spectrum. Then the value ΔE will be in the range of 42–51 meV for non-annealed films, and $\Delta E = 36$–38 meV for annealed films. In the graphs, the effect of the increase of the sharpness of the OT edge is clearly visible for films of the compositions $x = 0.60$ (Figure 1, *a*, spectra *1* and *2*, $T_{ann} = 370\,^{\circ}$C) and $x = 0.70$ (Figure 1, *b*, spectra *3* and *4*, $T_{ann} = 440\,^{\circ}$C). Figure 1, *a* also shows the OT spectra of samples of similar composition ($x = 0.63$) of a bulk CdHgTe crystal (spectrum *3*) and a layer grown by the LPE method on a CdTe substrate (spectrum *4*). It can be seen that the slope of the OT edge of the annealed film with $x = 0.60$ grown by the MBE method corresponds to that of the layer grown by the LPE method ($\Delta E = 35$ meV), and the slope of the edge of the bulk sample ($\Delta E = 26$ meV) is still sharper. Thus, some equalization of the composition occurred in films grown by the MBE method as a result of annealing.

A shift of the OT edge was observed as a result of annealing in all films. Its value at half the signal intensity is shown in Table 1.

PL spectra were recorded at $T = 103$ K and $T = 294$ K. Figure 2 shows the PL spectra of a number of films of various compositions before and after thermal annealing recorded at $T = 103$ K. The shallow levels (with the energy $E_s \leq 15$ meV) at this temperature which are sometimes observed at $T = 4.2$ K [11], are already ionized, and the spectra contained only one „edge“ band. Another type of levels observed in films grown with this MBE technology, — deep, with $70 \leq E_d \leq 90$ meV [11], was not detected in the studied samples. The full width at half-maximum (FWHM) of PL bands of films with compositions $x = 0.50$, $x = 0.60$ and $x = 0.70$ grown in one series of experiments at $T = 103$ K were 19, 28 and 40 meV before annealing, respectively. FWHM of bands were ~ 40 meV

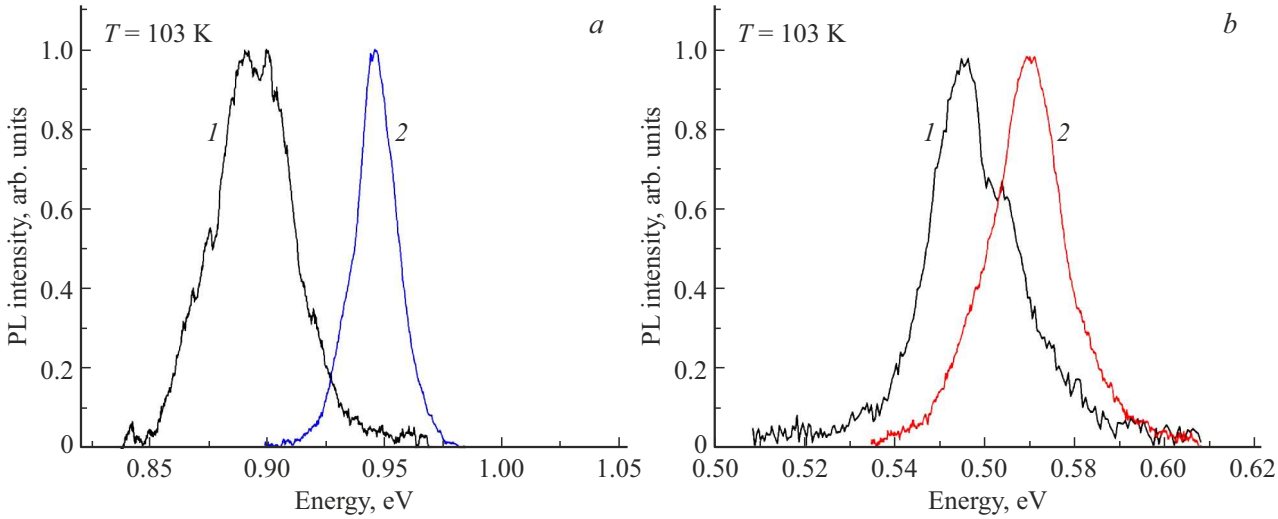

Figure 2. Normalized photoluminescence spectra of films with $x = 0.70$ (*a*) and $x = 0.50$ (*b*) before (*1*) and after (*2*) annealing performed at temperatures of 440 °C (*a*) and 370 °C (*b*).

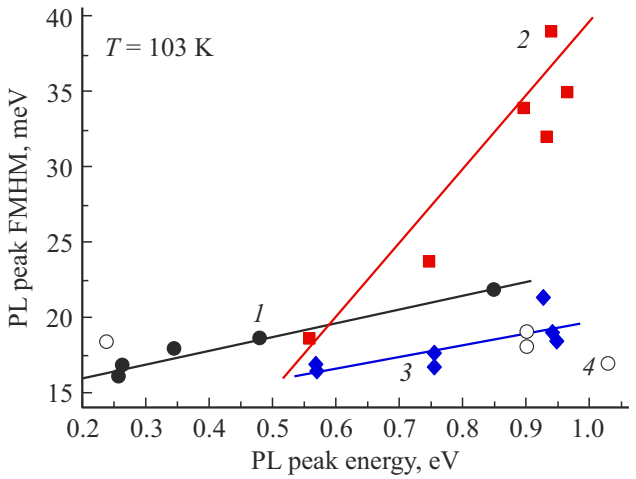

Figure 3. The ratios between the energies and FWHMs of the PL peaks for CdHgTe samples grown by the volumetric growth method (*1*), MBE (*2* — non-annealed and *3* — annealed), and LPE (*4*).

at $T = 294$ K for films with $x = 0.50$ and $\sim 55-58$ meV for films with $x = 0.60$ and $x = 0.70$. A shift of the maximum of the PL band towards high energies and a decrease in FWHM were observed after thermal annealing; these values for $T = 103$ K and $T = 294$ K are presented in Table 1. For a film with $x \approx 0.7$ annealed for comparison in the annealing mode to minimize the vacancy concentration (24 h in saturated mercury vapor at $T_{ann} = 225$ °C), the shift of the PL peak was insignificant, but its FWHM also decreased from ~ 30 to ~ 20 meV.

Figure 3 shows the relationship between the FWHMs of the PL peaks and the energies of these peaks (i. e., indirectly, the value x) at $T = 103$ K. The straight lines in Figure 3 represent linear approximations of some relations and are given for clarity. It can be seen that FWHM of the PL peaks for samples of bulk crystals (symbols *1*) slightly increases with an increase of x. A sharp increase of FWHM is observed in non-annealed films grown by the MBE method (symbols *2*) with an increase of x; at the same time, the FWHM values themselves significantly exceed those for bulk crystals (symbols *1*) and layers grown using the LPE method (characters *4*). The dependence of FWHM on the composition becomes weak for annealed films grown by the MBE method (symbols *3*), and the FWHM values themselves become comparable to those for bulk material and layers grown by the LPE method.

X-ray diffraction studies were performed for films with $x = 0.70$ (before and after annealing at $T_{ann} = 440$ °C) and $x = 0.50$ (non-annealed film). Diffraction patterns obtained in a wide slit configuration (1.0 mm equatorial slits were used) are shown in Figure 4 and generally have a similar appearance. The main peak of the XRD at angles $\sim 97.8°$ had a complex structure, here the two main peaks for the film with $x = 0.70$ (angles 97.61° and 97.93°) corresponded to the CdHgTe with $x \approx 0.7$ (tabular the value for $Cd_{0.7}Hg_{0.3}Te$(620) 97.64°; the peak at 97.93° most likely corresponded to the radiation of $K\alpha_2$). The peak at the angle 85.70° had a low intensity and was excluded from the analysis. The XRD rocking curves (RCs) were obtained in a narrow slit configuration (0.05 mm equatorial slits were used); their FWHMs are shown in Table 2.

The diffraction pattern of the annealed structure with $x = 0.70$, in addition to the XRD peaks from $Cd_{0.7}Hg_{0.3}Te$, discussed above, contained a peak at an angle of 119.05°, which could be attributed to diffraction from the substrate (tabular value for GaAs (620) 119.07°). This indicated a lower angle of misorientation of the crystallographic directions of the film and substrate compared to the non-annealed sample (in the initial sample, it was estimated as $\sim 0.7°$). There was no such peak on the diffraction pattern

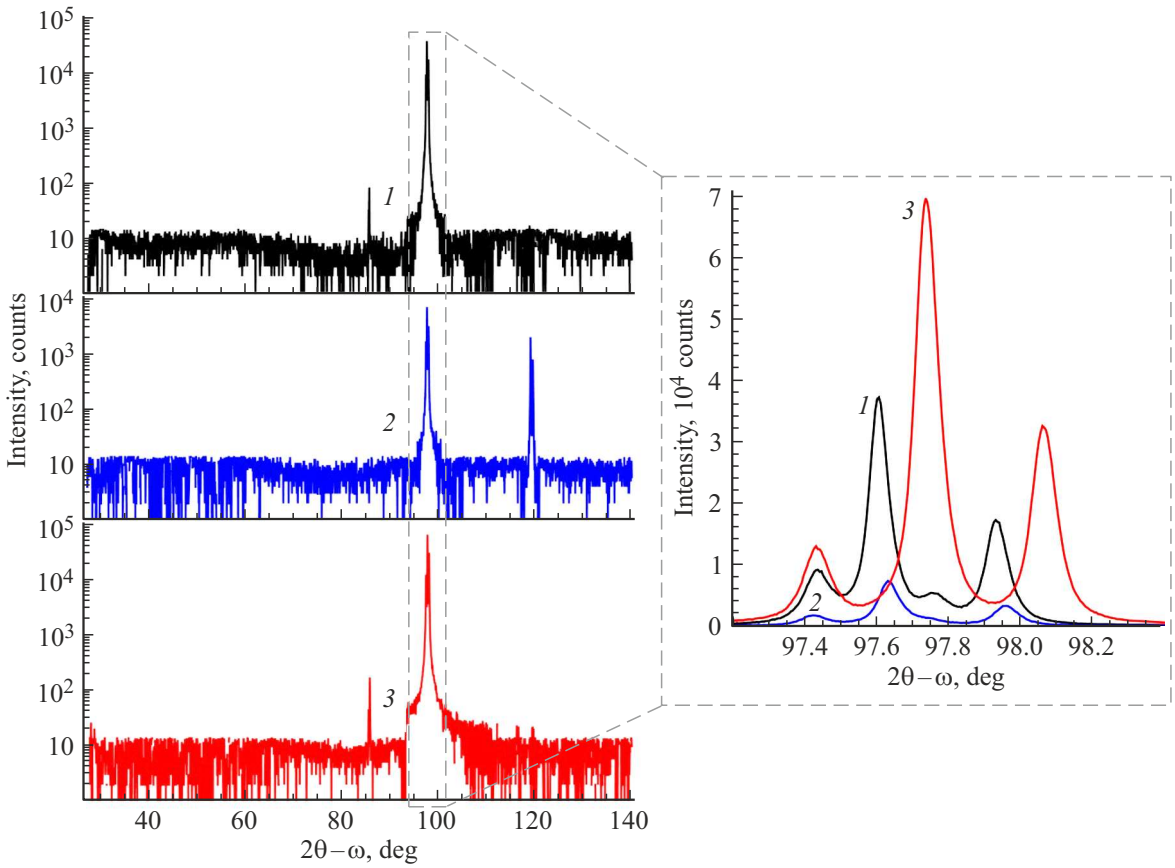

Figure 4. X-ray diffraction spectra of films with $x = 0.70$ before (*1*) and after (*2*) annealing at $T_{ann} = 440\,^{\circ}\mathrm{C}$ and non-annealed film with $x = 0.50$ (*3*). The callout shows peaks near the angle 97.6 °.

Table 2. FWHMs of the XRD RCs of the studied samples

Film composition	Half-width of the RC angular seconds
$x = 0.70$ (not annealed), $2\theta = 97.61^{\circ}$	119
$x = 0.70$ (after annealing), $2\theta = 97.63^{\circ}$	173
$x = 0.50$ (not annealed), $2\theta = 97.74^{\circ}$	176

of the non-annealed film with $x = 0.50$ (curve *3*, here the angle of misorientation was estimated as $\sim 0.9^{\circ}$). The main XRD peaks from the film here corresponded to the angles 97.74° and 98.07°; the FWHM of the XRD RC for this sample is also shown in Table 2.

Thus, the XRD data showed the crystallinity of the films both before and after annealing. Annealing of the film with $x = 0.70$ led to a decrease of the intensity of peaks and a broadening of the XRD RC, but at the same time the misorientation of the film and substrate significantly decreased, and the parasitic XRD peak disappeared at an angle of 85.70°. A decrease of the intensity of the XRD signal after annealing has already been observed by us in films with $x = 0.74$ and $x = 0.38$ [12]; this effect may be caused by a decrease of the size of coherent scattering regions caused by the accumulation of point defects on the extended ones due to the diffusion of the first during the annealing process.

According to the XRD data, the diffraction peak from the film with $x = 0.70$ shifted to the region of large angles as a result of annealing. This effect indicates a change of the interplane distance as a result of annealing, which could be associated with either a change (in this case, a decrease) in x or relaxation processes in the film and its deformation. This film was additionally investigated by the EDX method to analyze the change of x as a result of annealing. The studies used an accelerating voltage of 10 kV at normal electron beam incidence, which, according to estimates made using the CASINO [13] program, corresponded to the thickness of the signal generation region ~ 250 nm. Measurements carried out at five points on the surface of each sample showed the component content for the non-annealed film corresponding to $x = 0.65$; the composition of the film after annealing was estimated as $x = 0.67$. No foreign chemical elements were detected. The deviation of the composition of the CdHgTe films determined by the EDX method to a smaller side relative to the values of x obtained by OT and *in situ* ellipsometry is typical for the applied technique [10]. This may be attributable to the shallow penetration depth of the electron beam and an

increase of the mercury concentration on the film surface as a result of its oxidation. Qualitatively, the EDX data confirmed the results of optical studies, which showed an increase of x as a result of annealing.

Thus, as before in case of the film with $x = 0.74$ [12], the XRD studies conducted in the framework of this paper did not reveal significant changes in the crystalline perfection of the CdHgTe, even after high-temperature (at 440 °C) annealing. At the same time, optical research data showed an improvement (in the form of an increase of the sharpness of the OT edge and a narrowing of the half-width of the PL spectra) in the quality of the material, as well as a change of x. It should be noted that according to the XRD data, the studied films with $x = 0.70$ had higher crystal perfection both before and after annealing compared to the film with $x = 0.50$ (see Table 2), while the film with $x = 0.50$ had the best quality according to the OT (Figure 1, *b*) and PL data (Figure 2). Thus, it is obvious that the effects observed in the OT and PL experiments were mainly the result of point defect diffusion rather than structural changes. The key factor in the changes of optical properties here was the annealing temperature, which is higher for films with a large x, and the mercury out-diffusion process was the main driving force. Indeed, experiments on annealing films with $x = 0.70$ in the above-described mode of minimizing the concentration of vacancies with a thin (50 nm) layer of HgTe deposited on the surface showed a shift in the edge of the OT at $T = 294$ K and the peak of the PL at $T = 103$ K at 10–15 meV towards low energies, which was obviously attributable to the reverse process, such as the diffusion of mercury from HgTe into CdHgTe.

For CdHgTe grown by equilibrium methods (volumetric growth and LPE), the manifestation in the optical properties of the effect of a noticeable change in x as a result of annealing is generally atypical of [14], while this effect has been observed repeatedly for films grown by MBE and vapor-phase epitaxy using organometallic compounds [14,15]. Most likely, it is associated with a significant initial disordering of such materials. If in the material grown by vapor-phase epitaxy using organometallic compounds, this disorder is caused by a layered structure (alternating layers of HgTe and CdTe during growth), then in films grown by the MBE method, it can be explained by a large scale of fluctuations in chemical composition. The diffusion of point defects during annealing under such conditions significantly changes optical properties, practically without affecting the structural properties. These effects should be taken into account when designing the appropriate structures: the key attention during annealing should be paid to changes of the optical properties of the material in the manufacture of photodetectors (shift of the absorption edge, see, for example, [15]), while in the manufacture of quantum-well injection laser, to the chemical composition of the barrier layer, which determines the electronic structure, and, accordingly, the rate of Auger recombination [16].

The generation of acceptor states in the studied samples as a result of annealing will be considered in the next study.

Conclusion

The structural and optical properties of $Hg_{1-x}Cd_xTe$ films with a high ($x = 0.5–0.7$) CdTe content grown by molecular beam epitaxy were studied using optical transmittance, photoluminescence, X-ray diffraction, and energy dispersive X-ray spectroscopy before and after thermal annealing. The XRD studies did not reveal significant changes in the crystalline perfection of the films after annealing, but optical research data showed a significant improvement (in the form of an increase of the sharpness of the OT edge and a narrowing of the FWHM of the PL spectra) in the quality of the material, as well as a change of its average chemical composition. These effects are explained by the presence of significant fluctuations in the chemical composition, which determined the specifics of the diffusion of point defects during annealing.

Acknowledgments

The authors would like to thank Y.D. Kirilenko for his help in analyzing the results of EDX.

Funding

The work in the field of structure growth, thermal annealing, and optical transmittance research was partially supported by the Russian Science Foundation grant No. 24-62-00010.

Conflict of interest

The authors declare that they have no conflict of interest.

References

[1] T. Le Goff, T. Pichon, N. Baier, O. Gravrand, O. Boulade. J. Electron. Mater. **51**, *10*, 5586 (2022).
[2] V.V. Rumyantsev, K.A. Mazhukina, V.V. Utochkin, K.E. Kudryavtsev, A.A. Dubinov, V.Ya. Aleshkin, A.A. Razova, D.I. Kuritsin, M.A. Fadeev, A.V. Antonov, N.N. Mikhailov, S.A. Dvoretsky, V.I. Gavrilenko, F. Teppe, S.V. Morozov. Appl. Phys. Lett. **124**, *16*, 161111 (2024).
[3] M. Vallone, M. Alasio, A. Tibaldi, F. Bertazzi, S. Hanna, A. Wegmann, D. Eich, H. Figgemeier, G. Ghione, M. Goano. IEEE Photon. J. **16**, *1*, 6800208 (2024).
[4] A.V. Voitsekhovskii, S.M. Dziadukh, D.I. Gorn, N.N. Mikhailov, S.A. Dvoretsky, G.Yu. Sidorov, M.V. Yakushev. J. Opt. Technol. **91**, *2*, 67 (2024).
[5] G.A. Umana-Membreno, H. Kala, S. Bainsy, N.D. Akhavan, J. Antoszewski, C.D. Maxey, L. Faraone. J. Electron. Mater. **45**, *9*, 4686 (2016).
[6] K. Majkowycz, K. Murawski, M. Kopytko, Infr. Phys. Technol. **137**, 105126 (2024).
[7] D. Shaw, P. Capper. In: Mercury Cadmium Telluride: Growth, Properties, and Applications / eds. P. Capper, J. Garland. John Wiley & Sons Ltd., Chichester (2010). P. 297.
[8] V.A. Shvets, N.N. Mikhailov, D.G. Ikusov, I.N. Uzhakov, S.A. Dvoretsky. Opt. Spectroscopy **127**, *2*, 340 (2019).

[9] F.-Y. Yue, S.-Y. Ma, J. Hong, P.-X. Yang, C.-B. Jing, Y. Chen, J.-H. Chu. Chin. Phys. B **28**, *1*, 017104 (2019).
[10] M.S. Ruzhevich, K.D. Mynbaev, N.L. Bazhenov, M.V. Dorogov, V.S. Varavin, N.N. Mikhailov, I.N. Uzhakov, V.G. Remesnik, M.V. Yakushev. J. Opt. Technol. **91**, *2*, 77 (2024).
[11] M.S. Ruzhevich, K.D. Mynbaev, N.L. Bazhenov, M.V. Dorogov, S.A. Dvoretsky, N.N. Mikhailov, V.G. Remesnik, I.N. Uzhakov. Phys. Sol. State **65**, *3*, 402 (2023).
[12] K.D. Mynbaev, N.L. Bazhenov, A.M. Smirnov, N.N. Mikhailov, V.G. Remesnik, M.V. Yakushev. Semiconductors **54**, *12*, 1561 (2020).
[13] D. Drouin, A.R. Couture, D. Joly, X. Tastet, V. Almez, R. Gauvin. Scanning **29**, *3*, 92 (2007).
[14] M.S. Ruzhevich, K.D. Mynbaev. Rev. Adv. Mater. Technol. **2**, *4*, 47 (2020); **4**, *4*, 17 (2022).
[15] J. Sobieski, M. Kopytko, K. Matuszelanski, W. Gawron, J. Piotrowski, P. Martyniuk. Sensors **24**, 2837 (2024).
[16] M.A. Fadeev, A.A. Dubinov, V.Ya. Alyoshkin, V.V. Rumyantsev, V.V. Utochkin, V.I. Gavrilenko, F. Tepe, H.-V. Hubers, N.N. Mikhailov, S.A. Dvoretsky, S.V. Morozov. Quant. Electron. **49**, *6*, 556 (2019).

Translated by A.Akhtyamov